ATHEROSCLEROSIS

Detecting human coronary inflammation by imaging perivascular fat

Alexios S. Antonopoulos,[1]* Fabio Sanna,[1]* Nikant Sabharwal,[2] Sheena Thomas,[1] Evangelos K. Oikonomou,[1] Laura Herdman,[1] Marios Margaritis,[1,3] Cheerag Shirodaria,[2] Anna-Maria Kampoli,[1] Ioannis Akoumianakis,[1] Mario Petrou,[4] Rana Sayeed,[4] George Krasopoulos,[4] Constantinos Psarros,[1] Patricia Ciccone,[1] Carl M. Brophy,[1] Janet Digby,[1] Andrew Kelion,[2] Raman Uberoi,[5] Suzan Anthony,[5] Nikolaos Alexopoulos,[6] Dimitris Tousoulis,[6] Stephan Achenbach,[7] Stefan Neubauer,[1,3,8] Keith M. Channon,[1,3,8] Charalambos Antoniades[1,3,8†]

Early detection of vascular inflammation would allow deployment of targeted strategies for the prevention or treatment of multiple disease states. Because vascular inflammation is not detectable with commonly used imaging modalities, we hypothesized that phenotypic changes in perivascular adipose tissue (PVAT) induced by vascular inflammation could be quantified using a new computerized tomography (CT) angiography methodology. We show that inflamed human vessels release cytokines that prevent lipid accumulation in PVAT-derived preadipocytes in vitro, ex vivo, and in vivo. We developed a three-dimensional PVAT analysis method and studied CT images of human adipose tissue explants from 453 patients undergoing cardiac surgery, relating the ex vivo images with in vivo CT scan information on the biology of the explants. We developed an imaging metric, the CT fat attenuation index (FAI), that describes adipocyte lipid content and size. The FAI has excellent sensitivity and specificity for detecting tissue inflammation as assessed by tissue uptake of 18F-fluorodeoxyglucose in positron emission tomography. In a validation cohort of 273 subjects, the FAI gradient around human coronary arteries identified early subclinical coronary artery disease in vivo, as well as detected dynamic changes of PVAT in response to variations of vascular inflammation, and inflamed, vulnerable atherosclerotic plaques during acute coronary syndromes. Our study revealed that human vessels exert paracrine effects on the surrounding PVAT, affecting local intracellular lipid accumulation in preadipocytes, which can be monitored using a CT imaging approach. This methodology can be implemented in clinical practice to noninvasively detect plaque instability in the human coronary vasculature.

INTRODUCTION

Inflammation is a key feature in atherogenesis (*1*), and modalities that can accurately detect vascular inflammation would enable better cardiovascular risk stratification and implementation of appropriate preventive strategies. Inflammation also characterizes vulnerable atherosclerotic plaques, the rupture of which leads to major cardiovascular events such as acute coronary syndromes and ischemic strokes (*1*). Noninvasive detection of vascular inflammation has been hailed as the "holy grail" in cardiovascular medicine, because it would allow identification of patients at high risk for future cardiovascular events and initiation of appropriate risk reduction strategies. Current tools to assess vascular inflammation that rely on systemic plasma biomarkers (high-sensitivity C-reactive protein and proinflammatory cytokines) are not directly related to the process of atherogenesis, do not identify vulnerable atherosclerotic plaques, and provide very poor associations with local vascular biological processes (*2*, *3*). Moreover, existing invasive (intravascular ultrasound and optical coherence tomography) and noninvasive [computerized tomography angiography (CTA) or 18F-fluorodeoxyglucose (^{18F}FDG)–positron emission tomography (PET)] imaging tools cannot provide reliable information on vascular inflammation in human coronary arteries (*4*). Coronary calcium scoring (CCS) is the only established noninvasive imaging biomarker with predictive value in primary prevention (*5*), but it describes nonreversible structural changes of the vascular wall, and it is not altered by interventions that reduce cardiovascular risk such as statins. An imaging biomarker that could overcome these limitations and noninvasively detect vascular inflammation would be invaluable in clinical research, risk stratification of coronary artery disease (CAD), and identification of patients at high risk of future cardiovascular events (*6*).

Adipose tissue releases a wide range of bioactive molecules that exert endocrine and paracrine effects on the vascular wall (*7*), and we have recently shown that the communication between adipose tissue and the vascular wall is bidirectional (*3*, *8*). The biological properties of adipose tissue are largely driven by the degree of differentiation of small, immature preadipocytes to large, well-differentiated adipocytes rich in intracellular lipid droplets (*9*). The differentiation of immature preadipocytes is promoted by *PPAR*-γ activation, but this mechanism is suppressed by exogenous inflammation (*10*). Currently, there is no established noninvasive method to monitor adipocyte lipid content in human adipose tissue, although the correlation between adipocyte size and the balance between the lipid and aqueous phases of adipose tissue (*11*) may lend itself to detection by imaging modalities such as CT. Hence, information about composition of tissues could provide indirect information on adipocyte size, a concept that has not been explored.

We hypothesized that the phenotypic characterization of human adipose tissue could be accomplished in a noninvasive manner by using CT imaging to assess adipocyte lipid content and that coronary perivascular adipose tissue (PVAT) would function as a sensor rather than

[1]Division of Cardiovascular Medicine, Radcliffe Department of Medicine, University of Oxford, Oxford, UK. [2]Cardiothoracic Directorate, Oxford University Hospitals National Health System (NHS) Foundation Trust, Oxford, UK. [3]Oxford Centre of Research Excellence, British Heart Foundation, Oxford, UK. [4]Department of Cardiothoracic Surgery, Oxford University Hospitals NHS Foundation Trust, Oxford, UK. [5]Department of Radiology, Oxford University Hospitals NHS Foundation Trust, Oxford, UK. [6]1st Department of Cardiology, Athens University Medical School, Athens, Greece. [7]Medizinische Klinik 2, Universitätsklinikum Erlangen, Erlangen, Germany. [8]Oxford Biomedical Research Centre, National Institute of Health Research, Oxford, UK.
*These authors contributed equally to this work.
†Corresponding author. Email: antoniad@well.ox.ac.uk

a driver of coronary inflammation. We further hypothesized that if vascular inflammation prevents lipid accumulation in preadipocytes of PVAT through paracrine signaling mechanisms, then it may also lead to changes in tissue composition that could be detectable by high-resolution CTA. This approach would therefore permit detection of both inflamed coronary arteries without atherosclerosis and vulnerable atherosclerotic plaques prone to rupture, which would have important ramifications for patient management.

RESULTS

Characterizing adipocyte size and lipid content in different adipose tissue depots

The study flow chart is presented in fig. S1. We first studied the phenotypic differences between epicardial (EpAT), thoracic (ThAT), and subcutaneous (ScAT) adipose tissue obtained from 453 patients undergoing cardiac surgery (study arm 1; table S1). EpAT and ThAT had smaller adipocytes and increased adipocyte number compared to ScAT (Fig. 1, A to E). In a proof-of-principle experiment, we demonstrated that maturation of adipocytes is directly linked to lipid accumulation and down-regulation of preadipocyte secreted factor (pref-1) that inhibits adipogenesis (fig. S2), resulting in increased adipocyte size that can be reliably tracked by fatty acid binding protein-4 (*FABP4*) gene expression (Fig. 1F). Fat depots with larger adipocytes, such as ScAT, had higher *PPAR*-γ [an adipocyte early-phase differentiation marker (*9*)] (Fig. 1G), CCAAT/enhancer binding protein (C/EBP) α [*CEBPA*, an adipocyte late-phase differentiation marker (*9*)] (Fig. 1H), and *FABP4* (a marker of terminal adipocyte differentiation/mature adipocytes) gene expression (Fig. 1I). These findings confirmed the notion that the expression of *FABP4*, *CEBPA*, and *PPAR*-γ genes could be used as markers of adipocyte size (*12*).

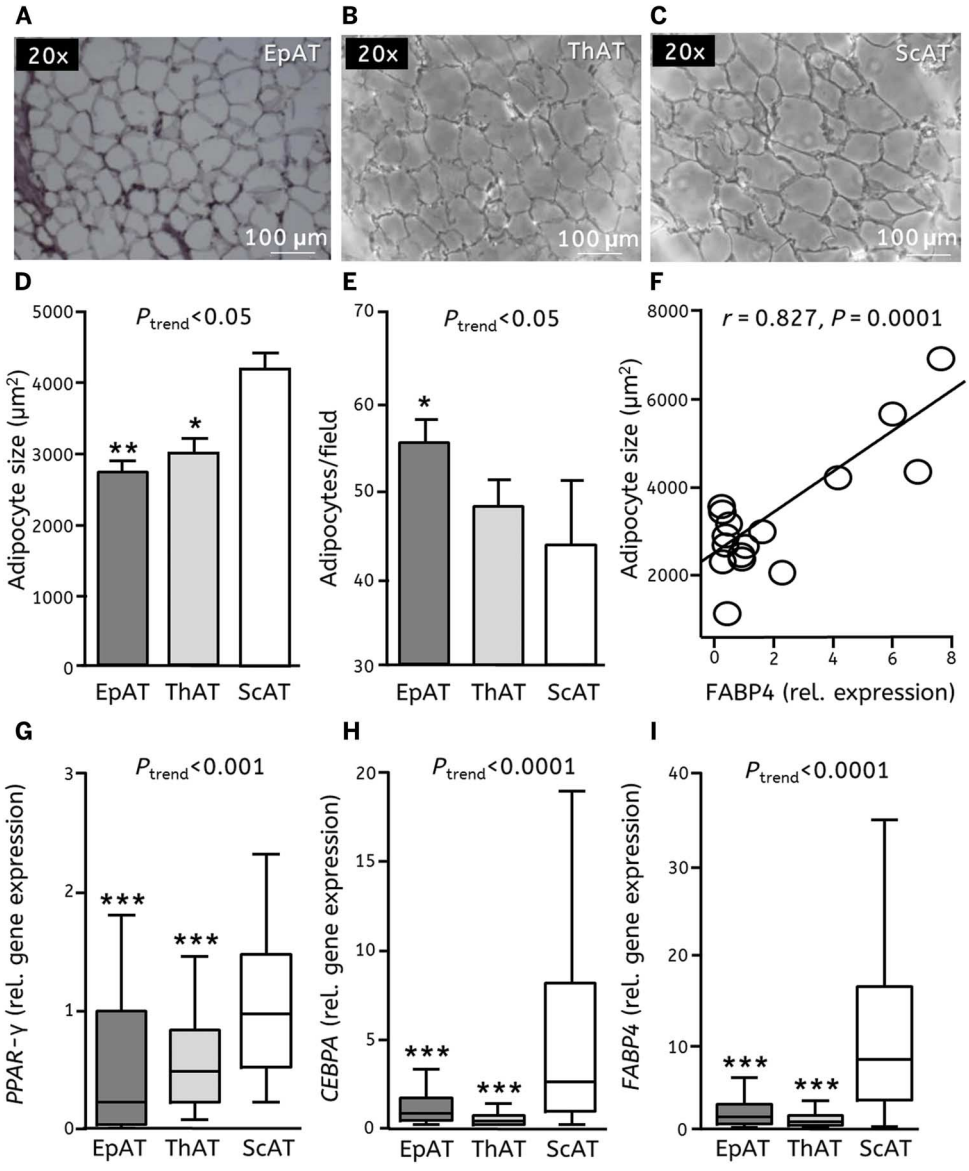

Fig. 1. Phenotyping of human adipose tissue. Representative bright-field microscopic images of human (**A**) EpAT, (**B**) ThAT, and (**C**) ScAT. (**D**) Adipocyte size (n = 5 patients) and (**E**) adipocytes per field (n = 6 patients), quantified from tissue sections of EpAT, ThAT, and ScAT from the same patients. (**F**) Adipocyte size correlated with *FABP4* expression (n = 16). (**G**) Gene expression of *PPAR*-γ, (**H**) *CEBPA*, (**I**) and *FABP4* (samples from n = 433 patients). P_{trend} derived from repeated-measures analysis of variance (ANOVA) with Bonferroni correction (D), Friedman's test with Dunn's post hoc correction (E), or Kruskal-Wallis with Dunn's post hoc correction (G to I) *P < 0.05, **P < 0.01, ***P < 0.001 versus ScAT.

Effects of vascular inflammation on intracellular lipid accumulation of preadipocytes in human pericoronary adipose tissue

Our recent studies in humans (*3*, *8*) and additional evidence from animal studies (*13*) suggest that adipocytes in PVAT respond to proatherogenic processes in the underlying vascular wall that modify their biology. We assumed that inflammatory signals from the human arterial wall may diffuse into the PVAT to influence adipocyte lipid content by affecting biological processes such as adipocyte differentiation, proliferation, and lipolysis (*14*). Because fresh samples of native human coronary arteries are not easily obtained for research, we used aortic tissue harvested during coronary artery bypass grafting (CABG) surgery as our model. Aortic "buttons" obtained from the site of graft anastomosis on the ascending aorta from patients in study arm 2 (table S1) were cultured ex vivo for 1 week in the presence or absence of angiotensin II (100 nM) to induce vascular inflammation (Fig. 2A). Exposure to angiotensin II for 1 week led to up-regulation of the proinflammatory cytokines *IL-6*, *TNF*-α, and *IFN*-γ in the aortic tissue (Fig. 2B). The tissue was then washed to remove angiotensin II and cocultured with preadipocytes collected from the same patients, followed by induction of adipocyte differentiation to mature adipocytes using a well-established methodology (*15*). When cocultured with aortic tissue that was pretreated with angiotensin II, preadipocytes showed less

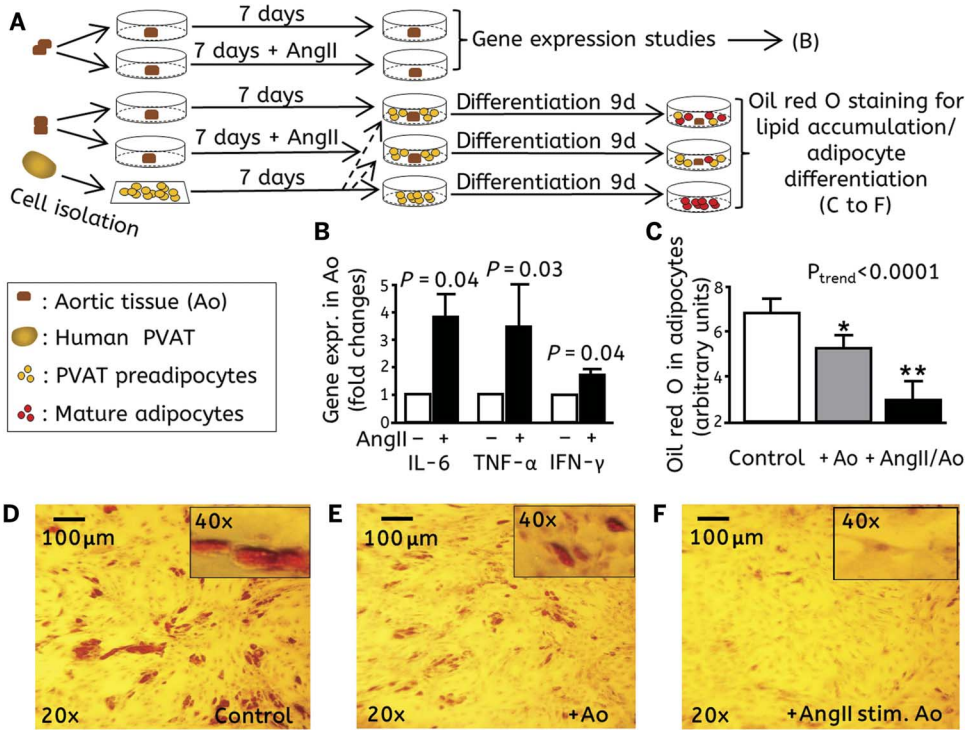

Fig. 2. Vascular inflammation blocks perivascular adipocyte differentiation through paracrine signals. (**A**) Experimental design of the coculture experiments in study arm 2. Human aortic tissue (Ao) from 15 patients undergoing CABG was harvested and cultured for 7 days ± angiotensin II (AngII; 100 nM). Preadipocytes isolated from PVAT around the right coronary artery (RCA) were also cultured for this period. After 7 days, the aortic tissue was washed to remove angiotensin II and was cocultured with the preadipocytes before a differentiation time course was induced. (**B**) *IL-6*, *TNF-α*, and *IFN-γ* gene expression in aortic tissue before and after stimulation with angiotensin II (n = 5 to 7 per group). (**C**) Quantification of oil red O in preadipocytes (control) or preadipocytes co-incubated with aortic tissue or aortic tissue prestimulated with angiotensin II (n = 6 per group). (**D** to **F**) Representative images of oil red O staining in preadipocytes co-incubated with aortic tissue as in (C). P values derived from Wilcoxon signed-rank test (B) and repeated-measures ANOVA followed by individual comparisons using paired t test (C). *P < 0.05, **P < 0.001 versus control.

intracellular lipid accumulation compared to preadipocytes cultured in the absence of aortic tissue, indicating slower differentiation to mature adipocytes; preadipocytes cocultured with nonstimulated aortic tissue had an intermediate amount of lipid accumulation (Fig. 2, C to F). This suggests that mediators released from the inflamed human vascular wall can exert paracrine effects on PVAT, altering its lipid content in part by preventing the differentiation of preadipocytes to mature adipocytes.

To explore whether inflammatory mediators produced in the vascular wall directly modify lipid accumulation in PVAT, we exposed human preadipocytes collected from PVAT to recombinant interleukin-6 (IL-6) + tumor necrosis factor–α (TNF-α) + interferon-γ (IFN-γ) and studied their differentiation in vitro. Exposure of preadipocytes to cytokines had an inhibitory effect on preadipocyte differentiation, as observed visually over time (fig. S3), and led to lower intracellular accumulation of lipid droplets (Fig. 3, A to E). The same cytokines also accelerated the proliferation of human preadipocytes, evaluated using the 3-(4,5-dimethylthiazol-2-yl)-5-(3-carboxymethoxyphenyl)-2-(4-sulfophenyl)-2*H*-tetrazolium (MTS) cell proliferation assay (Fig. 3F). The impact of these cytokines on preadipocyte differentiation was confirmed by quantifying the expression of *PPAR-γ*, *CEBPA*, and *FABP4* during the differentiation time course (Fig. 3, G to I). These findings support the notion that vessel-derived inflammatory cytokines inhibit lipid accumulation in PVAT by inducing the proliferation and inhibiting the differentiation of human preadipocytes in a paracrine manner. Therefore, we hypothesized that noninvasive imaging tools, capable of monitoring these phenotypic changes of PVAT driven by the underlying vascular inflammation, could be used to identify vascular inflammation in human coronary arteries.

Evaluating adipocyte lipid accumulation using CT

The balance between the lipid and aqueous phases of adipose tissue depends on adipocyte size (*11*) with larger adipocytes having increased lipid content and increased expression of *FABP4* (Fig. 1 and fig. S2). Because the CT attenuation of adipose tissue reflects the balance between lipid and aqueous phases, we concluded that adipose tissue CT attenuation may serve as a marker of adipocyte size/adipose tissue lipid content. To explore whether the average CT attenuation of adipose tissue provides a marker of average adipocyte size/adipose tissue lipid content, we quantified the fat attenuation index (FAI) in EpAT, ThAT, and ScAT explants obtained from 453 patients undergoing cardiac surgery (study arm 1). Briefly, the FAI is the average attenuation (reduction in signal) of adipose tissue within a volume of interest as measured from reconstructed CT. There was an inverse association between FAI and the degree of adipocyte differentiation as defined by the expression of *CEBPA* and *FABP4* in the same samples (Fig. 4, A to F, and table S2). However, FAI in EpAT did not correlate with the gene expression of *CD68*, a marker of macrophage infiltration (ρ = 0.180, P = 0.096) or the ratio of *CCR7* (macrophage marker of M1 polarization)/MRC1 (macrophage marker of M2 polarization) (ρ = −0.173, P = 0.109) (fig. S4). There was a weak but significant association between FAI in ScAT and ThAT explants and the ratio of *CCR7*/*MRC1* gene expression in the same samples (ρ = 0.182, P = 0.007 for ScAT and ρ = 0.191, P = 0.001 for ThAT), although there was no significant correlation between FAI and *CD68* gene expression in either ScAT (ρ = −0.116, P = 0.065) or ThAT (ρ = −0.078, P = 0.166) (fig. S4).

In addition, there was an inverse association between FAI of adipose tissue explants and adipocyte size quantified by histology (Fig. 4G). Accordingly, we established that FAI may be used as a marker of the variation of adipocyte size/adipose tissue lipid content in different depots: The greater the adipocyte differentiation/size, the more lipophilic the content of the tissue, therefore the more negative the FAI. To address this hypothesis in vivo, CT scans were performed in 105 patients (from study arm 1), aiming to link in vivo scan data with those from adipose tissue explants imaged ex vivo. We observed a correlation between the FAI obtained in vivo and the respective FAI measured in the explants of the same tissue that had been obtained from these patients (Fig. 4, H and I, and table S2).

To further validate the ability of FAI to estimate adipocyte lipid content in vivo, we correlated the in vivo FAI values for EpAT and ScAT

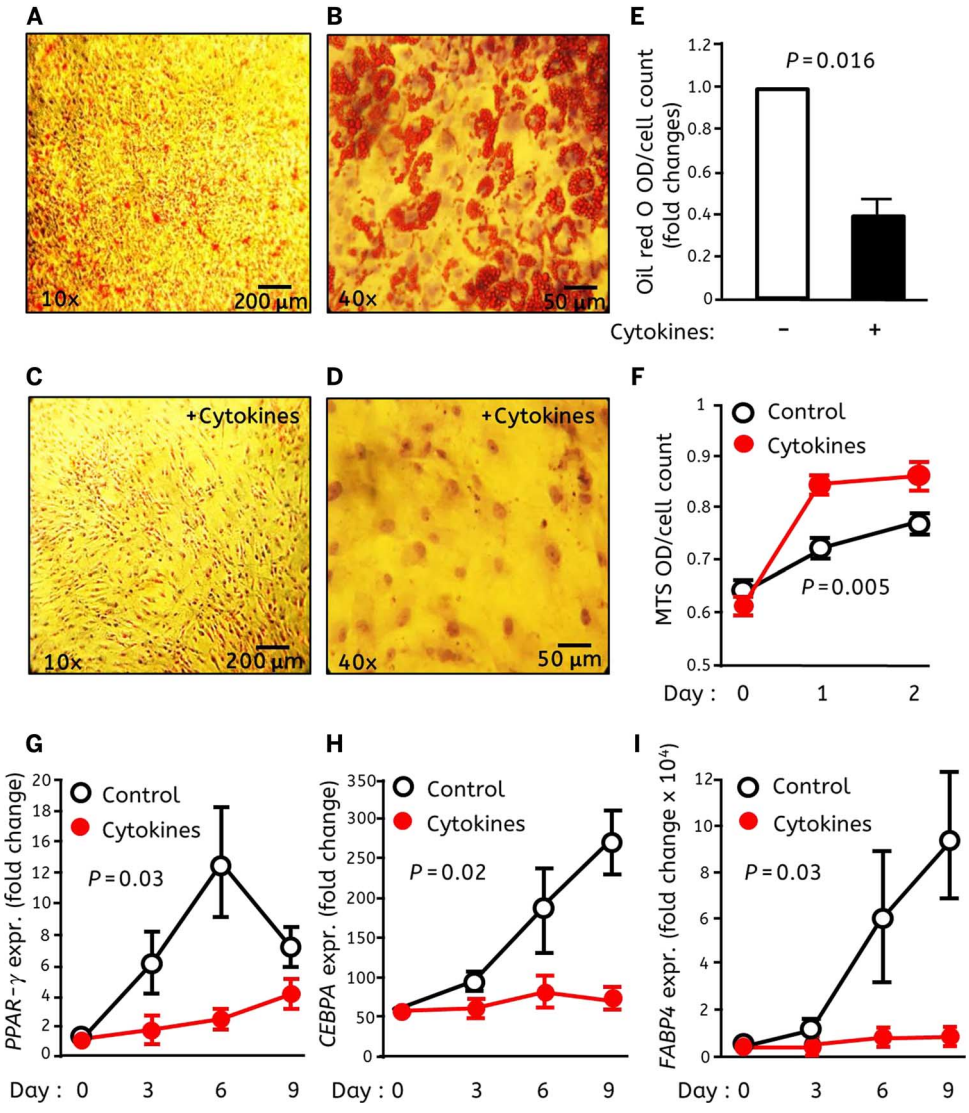

Fig. 3. Cytokines trigger proliferation and block differentiation of perivascular adipocytes. In study arm 2, human preadipocytes were isolated from PVAT around the RCA and differentiated in the presence or absence of inflammatory cytokines [recombinant TNF-α (4 ng/ml) + IL-6 (25 ng/ml) + IFN-γ (20 ng/ml)] until day 9 of differentiation [(**A** and **B**) without cytokines and (**C** and **D**) with cytokines, oil red O staining at day 9 of differentiation]. (**E**) Oil red O photometric quantification of lipid accumulation in preadipocytes differentiated with and without cytokines (n = 7). Effects of cytokines on (**F**) preadipocyte proliferation and gene expression of the differentiation markers (**G**) *PPAR-γ*, (**H**) *CEBPA*, and (**I**) *FABP4* (n = 3 independent experiments in triplicate). P values derived from Wilcoxon signed-rank test (E) or two-way ANOVA with "time × treatment" interaction (F to I).

from CT scans of the 105 patients in study arm 1 who also underwent a clinical CTA with the expression of adipocyte differentiation markers. We observed that in vivo FAI (table S2) was inversely related to the expression of both *CEBPA* (Fig. 5, A and B) and *FABP4* (Fig. 5, C and D) in the respective adipose tissue depots from these patients. FAI in EpAT (FAI_{EpAT}) in vivo was higher compared to FAI in ScAT (FAI_{ScAT}) in vivo (Fig. 5E), confirming that histologically demonstrated differences in differentiation status of adipose tissue depots led to respective differences in FAI in vivo. Homeostatic Model Assessment for Insulin Resistance (HOMA-IR), a marker of systemic insulin resistance that has been associated with increased adipocyte size (*16*), was negatively associated with FAI_{ScAT} in vivo but not with FAI_{EpAT} (Fig. 5F), suggesting that systemic metabolic status is linked to adipocyte lipid accumulation in isolated adipose tissue depots such as ScAT but not in EpAT or pericoronary adipose tissue. In addition to systemic insulin resistance, adipocyte lipid content was also affected by the extent of tissue infiltration by inflammatory cells such as activated macrophages. There was an inverse correlation between *CCR7*/*MRC1* gene expression ratio and *CEBPA* expression in ScAT (Fig. 6A) but not EpAT (Fig. 6B). In line with this finding, *CCR7*/*MRC1* ratio was positively associated with FAI in ScAT but not in EpAT (fig. S4), suggesting that FAI can be used as a surrogate marker of adipose tissue inflammation in isolated adipose tissue depots such as ScAT but not in EpAT where FAI seems to be regulated by local stimuli from the coronary arteries.

To further explore the ability of FAI to describe adipose tissue inflammation, we validated it against ^{18F}FDG uptake by adipose tissue using PET-CT imaging, which is the gold standard modality to noninvasively assess tissue inflammation in vivo (*4*). In a validation study undertaken in 40 subjects who had ^{18F}FDG PET-CT for a clinical indication, we assessed ^{18F}FDG uptake by ScAT using the PET images and FAI using the coupled CT images from the same scans. We observed a positive association between ^{18F}FDG uptake and FAI in ScAT (Fig. 6C), but there was no association between these two biomarkers in EpAT, a finding in line with the gene expression studies performed in the two adipose tissue depots. FAI_{ScAT} had excellent diagnostic accuracy for adipose tissue inflammation (defined using the median ^{18F}FDG uptake as a cutoff, TBR = 0.200). For a cutoff value of FAI_{ScAT} = 113.3 HU (Hounsfield units), high adipose tissue inflammation (TBR > 0.200) was detected with a sensitivity of 90% and a specificity of 100% (Fig. 6D). Representative images from a subject with high FAI_{ScAT}/high ^{18F}FDG uptake in ScAT and a subject with low FAI_{ScAT}/low ^{18F}FDG uptake in ScAT are presented in Fig. 6E.

Visualizing the changes in adipocyte size/adipose tissue lipid content in coronary PVAT in vivo

To investigate the relationship between FAI and adipocyte lipid content around the human coronary arteries, we compared adipose tissue obtained immediately adjacent to the RCA with adipose tissue obtained 2 cm away from the RCA and not in proximity with any visible epicardial coronary branch, from patients undergoing CABG in study arm 2. We observed that the expression of *PPAR-γ*, *CEBPA*, and *FABP4* was down-regulated closer to the RCA (Fig. 7, A to C), whereas there was no difference in the

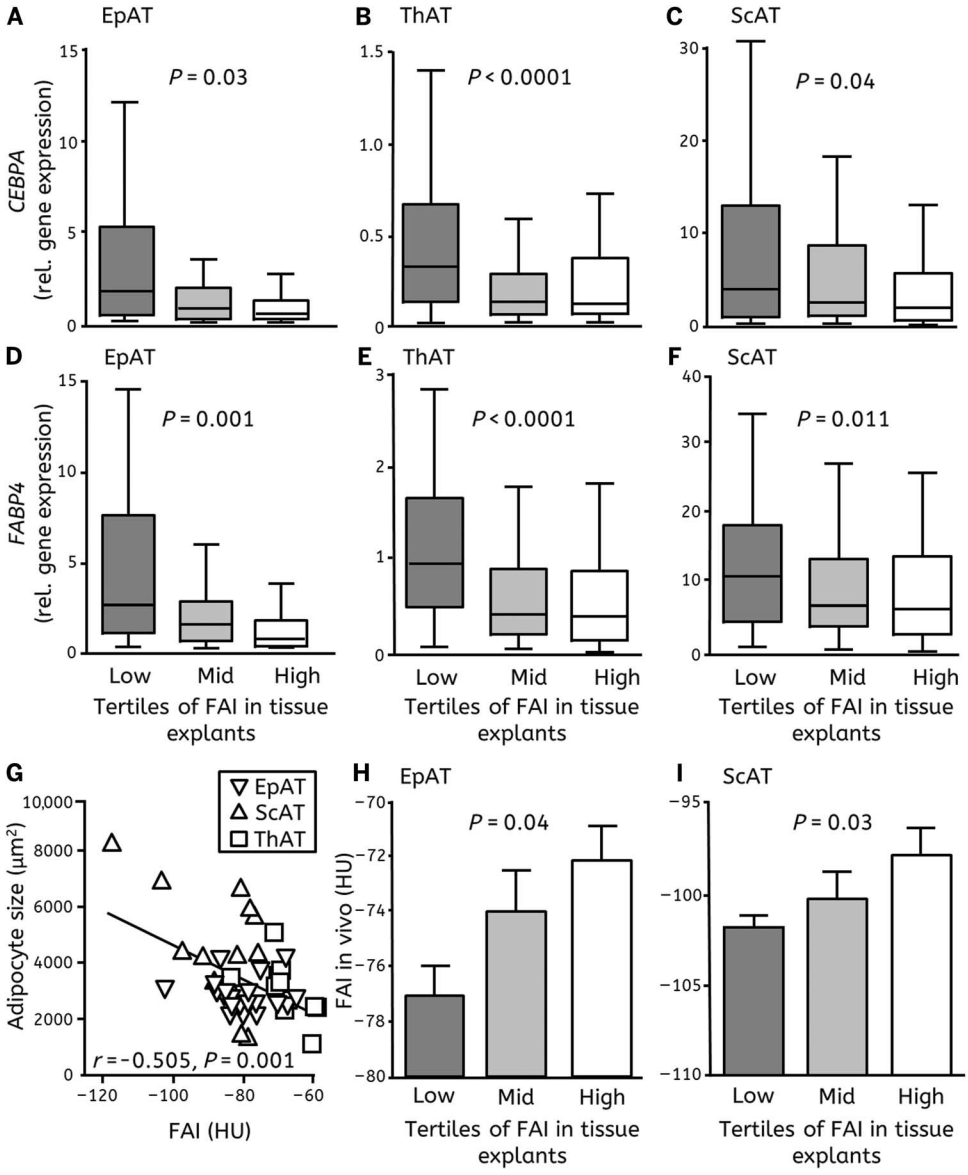

Fig. 4. Ex vivo characterization of adipocyte size and adipogenesis using CT. Explants of EpAT, ThAT, and ScAT from patients undergoing CABG (study arm 1) were scanned by CT to calculate FAI for each sample. Association of FAI with the expression of (**A** to **C**) *CEBPA* (EpAT, $n = 87$; ThAT, $n = 311$; ScAT, $n = 288$) and (**D** to **F**) *FABP4* (EpAT, $n = 85$; ThAT, $n = 312$; ScAT, $n = 259$) genes in all depots. (**G**) Correlation between adipocyte size and FAI ($n = 44$ biopsies). Association between FAI measured in vivo and in explants of (**H**) EpAT and (**I**) ScAT collected from 105 patients in study arm 1. *P* values by Kruskal-Wallis (A to F) and one-way ANOVA (H and I).

expression of inflammatory mediators within the tissue or macrophage infiltration and polarization (fig. S5). This was in line with the observed smaller adipocyte size in proximity to the RCA compared to an area 2 cm away from the vascular wall (Fig. 7D). These observations confirmed our findings from the ex vivo and in vitro experiments, suggesting that paracrine inflammatory signals from the human coronary artery rather than autocrine signals from within the tissue prevent lipid accumulation in PVAT surrounding them, although these effects are less marked as the distance from the RCA increases, even in the absence of obstructive vascular disease. To examine whether we could track these morphological changes of PVAT in response to coronary inflammation by noninvasive CT imaging, we used imaging analysis tools developed for the purpose of the study (UK Intellectual Property Office, application number 1414496.8) to analyze the CTA images of a clinical cohort of 273 subjects in study arm 3 (156 with and 117 without significant coronary plaques). We quantified FAI around the proximal segment of the RCA in three-dimensional cylindrical layers of 1-mm thickness, starting from the layer immediately adjacent to the vascular wall and moving up to 20 mm away from it (Fig. 7, E to G). FAI of PVAT (FAI_{PVAT}) calculation was feasible in all three major epicardial coronary arteries, but the RCA was used as a model to validate our ex vivo findings given the absence of major side branches and the ability to define PVAT versus non-PVAT, as well as the abundant amount of adipose tissue surrounding RCA, which can be easily harvested without major bleeding risk, in contrast to the other epicardial arteries. We observed a progressive decrease of FAI to more negative values as we moved away from the RCA—from PVAT to non-PVAT (Fig. 7, H and I), where adipocytes are larger (Fig. 7D) and better differentiated (Fig. 7, A to C). These findings suggest that the observed changes of FAI could detect the degree of vascular inflammation inside the human coronaries using a noninvasive approach in vivo.

Validating FAI against established imaging biomarkers and coronary atherosclerotic plaque burden

To validate FAI against established imaging biomarkers with known clinical predictive value, we quantified CCS in the RCA alone and the entire coronary vasculature, and atherosclerotic plaque burden in the proximal RCA in the 273 individuals of study arm 3 (table S3). The relationships between FAI and distance from the vascular wall were significantly ($P = 0.001$) different in patients with coronary atherosclerosis compared to healthy individuals (Fig. 7I), showing lower FAI values close to the vascular wall of healthy individuals. FAI in PVAT (FAI_{PVAT}, defined as the average FAI within a distance from the perimeter of the vessel equal to the diameter of the vessel) varied between patients even in the absence of coronary plaques (representative examples in fig. S6). There was also a significant ($P = 0.001$) difference in FAI_{PVAT} between patients with and without CAD independent of the presence of obstructive RCA disease (fig. S7), whereas there was no difference in $FAI_{non\text{-}PVAT}$ (defined as the FAI of an adipose tissue layer of 1-mm thickness, 2 cm away from the vascular wall) between CAD and non-CAD groups (Fig. 8A). When we examined the relationship between fat volumes and coronary atherosclerosis, we observed that EpAT volume was associated with total CCS, whereas PVAT volume

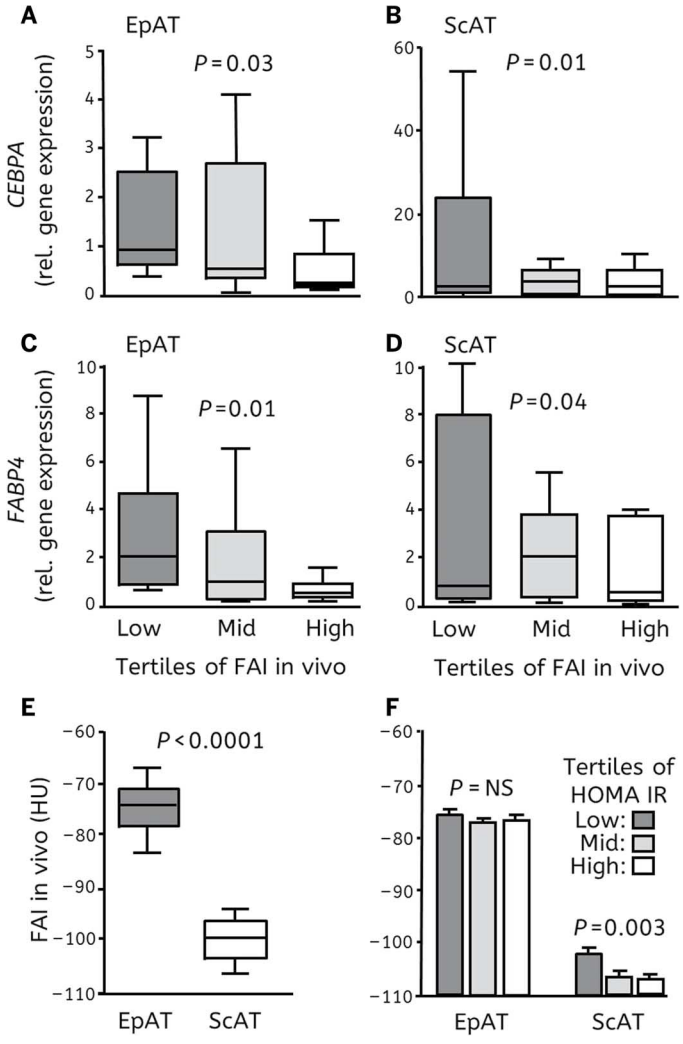

Fig. 5. In vivo characterization of adipogenesis by CT. Association of in vivo FAI for EpAT and ScAT of patients undergoing CT with gene expression of (**A** and **B**) *CEBPA* and (**C** and **D**) *FABP4* by the same adipose tissue samples collected from the same patients during surgery (study arm 1). (**E**) Comparison of in vivo FAI between EpAT and ScAT and (**F**) associations with systemic insulin resistance. *P* values by Kruskal-Wallis (A to D) or Wilcoxon signed-rank test (E) or one-way ANOVA (F). NS, Not significant. Studies were performed in the 105 patients from the in vivo CTA group of study arm 1.

around RCA was not associated with either the presence of CAD or the RCA calcium burden (fig. S8). There was a weak association between FAI_{PVAT} and total CCS or RCA CCS (fig. S9, A and B). To study whether the gradient of FAI from PVAT around the RCA to non-PVAT 20 mm away from the RCA provides additional information to FAI_{PVAT}, we calculated the volumetric perivascular characterization index (VPCI = $[100 \times (FAI_{PVAT} - FAI_{non\text{-}PVAT})/|FAI_{PVAT}|]$). This index should not be affected by systemic factors modifying global adipocyte size but would be mostly driven by local stimuli. VPCI was weakly associated only with the calcium burden in RCA but not total CCS (fig. S9, C and D). Neither FAI_{PVAT} nor VPCI was correlated with calcification volume in the underlying segment of the analyzed RCA (Fig. 8, B and C), suggesting that these imaging indices describe biological processes not directly related with local vascular calcium deposition. Both FAI_{PVAT} and VPCI were related to atherosclerotic plaque burden in the underlying RCA segment (Fig. 8, D and E), a finding which was similar for all major epicardial coronary arteries (fig. S10, B to D). VPCI was superior to FAI_{PVAT} in identifying noncalcified (soft) atherosclerotic lesions in the underlying coronary artery (Fig. 8F) but of moderate diagnostic value (fig. S11), suggesting that the current definition of vulnerable plaques as those without calcium does not accurately reflect the biological processes related to plaque rupture such as coronary plaque inflammation. To examine whether FAI_{PVAT} is related to the presence of CAD (defined as >50% stenosis in any coronary artery) independently of CCS, we performed multivariable linear regression in study arm 3, which showed that FAI_{PVAT} and CCS were related to the presence of CAD independently of each other and independently of age, gender, and other cardiovascular risk factors (table S4). Similarly, FAI_{PVAT} (but not total CCS in the entire coronary tree or CCS in the RCA) was positively related with atherosclerotic plaque burden of the RCA independently of age, gender, and cardiovascular risk factors (table S4).

Exploring the capacity of FAI to detect vascular inflammation and vulnerable atherosclerotic plaques

To further investigate the ability of FAI to detect dynamic changes in PVAT in response to variations in vascular inflammation, we studied FAI_{PVAT} around culprit lesions in patients with acute myocardial infarction (MI) within the past 72 hours. The CTA scans were performed immediately after percutaneous coronary intervention, where both culprit and obstructive nonculprit coronary lesions were treated in the same session. We observed that FAI_{PVAT} was increased by 8.76 ± 2.87 HU around the culprit lesion compared to FAI_{PVAT} proximal to the lesion (Fig. 8G). Because the CTA was performed after stent implantation in the culprit lesion, we then sought to examine whether the observed result was due to a possible artifact from the stent. As controls, we used the nonculprit lesions from the same patients where stent implantation was performed simultaneously with the culprit lesion, as well as stable patients who had received a coronary stent more than 3 months before the scan. An increase in $\Delta[FAI_{PVAT}]$ was observed around ruptured culprit lesions compared to either the nonculprit lesions in acute MI patients or lesions in stable CAD patients treated with a stent >3 months before the CTA (Fig. 8G); in the same patients, in a pooled analysis of all lesions, $\Delta[FAI_{PVAT}]$ was significantly ($P < 0.001$) increased around ruptured compared to stable plaques (Fig. 8H) and had high diagnostic accuracy for detecting these areas of vascular inflammation (Fig. 8I).

To examine whether FAI_{PVAT} around the culprit lesions of patients with recent MI changes over time, a subgroup of patients from the same cohort ($n = 5$) underwent further CTA 5 weeks post-MI. Patients with stable CAD ($n = 5$) were also rescanned 5 weeks after the first scan to act as a control group. There was a significant ($P = 0.04$) reduction in FAI_{PVAT} around the edges of the culprit lesion 5 weeks after the event, whereas there was no change in FAI_{PVAT} around the stable atherosclerotic plaques (Fig. 8J). Representative examples of differences in FAI_{PVAT} around a culprit stented lesion, a nonculprit stented lesion, a nontreated plaque, and a stent are provided (Fig. 8K).

DISCUSSION

Here, we present a method for detecting coronary inflammation by characterizing the changes in pericoronary adipose tissue CT attenuation. In a large cohort of patients undergoing cardiac surgery, we demonstrate that the average attenuation of adipose tissue (FAI) is inversely correlated with the expression of adipogenic genes and average adipocyte

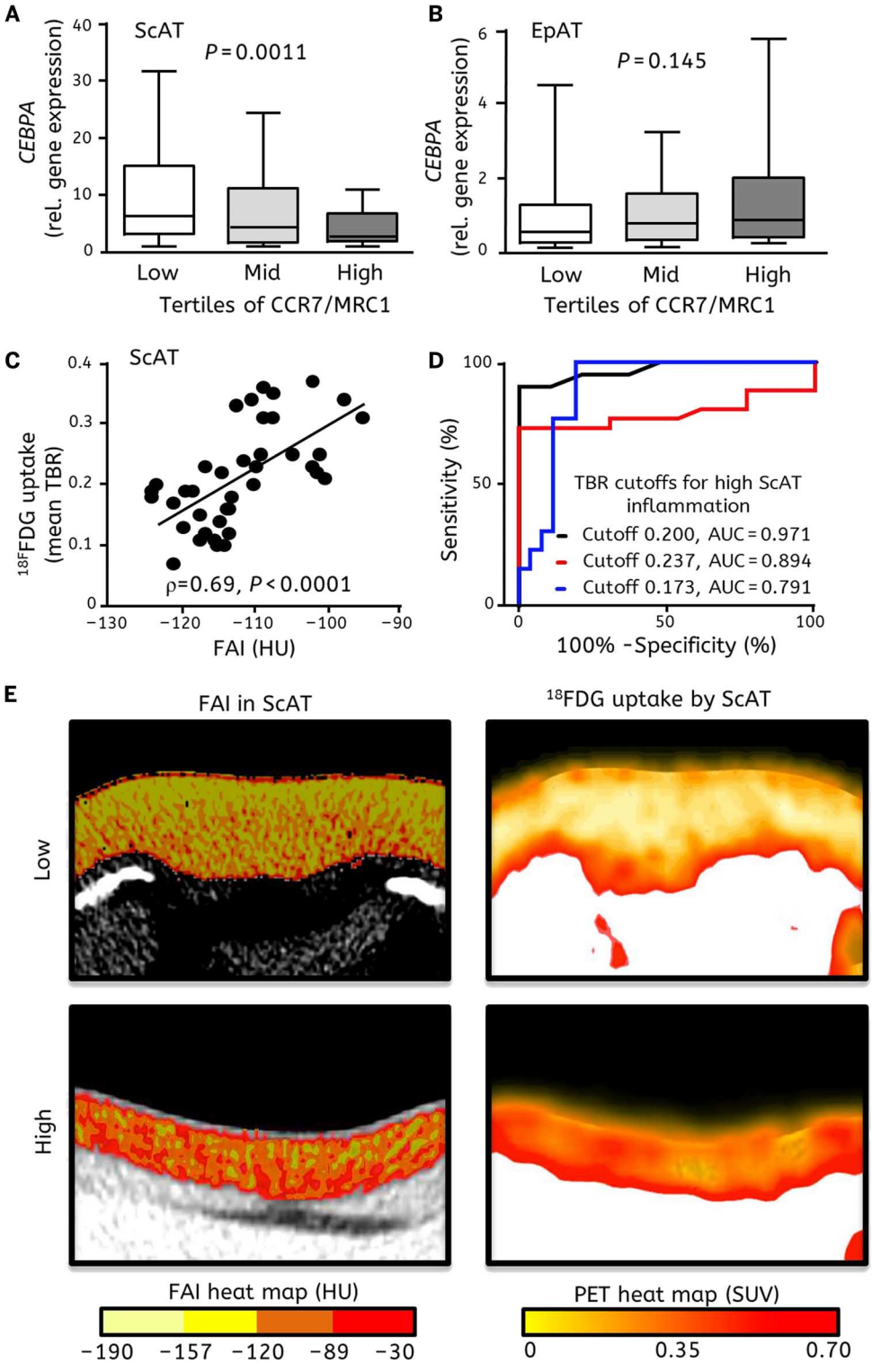

Fig. 6. FAI for the detection of human adipose tissue inflammation by noninvasive imaging. Associations between *CEBPA* gene expression and *CCR7/MRC1* gene expression ratio in (**A**) ScAT (n = 267) or (**B**) EpAT (n = 207) adipose tissue in study arm 1. (**C**) Correlations between ^{18F}FDG uptake of ScAT by PET/CT [determined as the mean tissue-to-background ratio (TBR)] with FAI of the same tissue (n = 39) and (**D**) receiver operating characteristic curves for identification of highly inflamed ScAT by FAI according to ^{18F}FDG uptake measured by PET/CT. (**E**) Representative examples of FAI and ^{18F}FDG uptake heat maps in ScAT. P values by Kruskal-Wallis test (A and B). SUV, standardized uptake value.

size, which is driven by intracellular lipid accumulation. We also show that the expression of adipogenic genes, the average adipocyte size, and lipid accumulation in PVAT are all driven by paracrine inflammatory signals from the vascular wall and are highly influenced by the presence of vascular disease. Using imaging tools developed for this purpose, we provide evidence that these biological effects of vascular inflammation on PVAT can be tracked by analyzing standard imaging sequences obtained during CTA. This concept is summarized in a schematic (Fig. 8L). On the basis of this approach, we provide imaging phenotyping that describes the degree of coronary artery inflammation, discriminates ruptured from nonruptured coronary atherosclerotic plaques during acute coronary syndromes, and describes coronary atherosclerotic plaque burden independently of CCS.

Adipose tissue contains adipocytes of varying sizes and differentiation status (*9*). Induction of adipocyte differentiation in the adipose tissue includes postconfluent mitosis and growth arrest of preadipocytes, which is essential for their subsequent differentiation to mature adipocytes. *PPAR-γ* and *CEBPA* are synergistically and cooperatively responsible for the early and intermediate phases of differentiation of preadipocytes and their subsequent entry into the terminal differentiation phase to mature adipocytes (*9*). In this latter phase, mature adipocytes are characterized by the expression of adipocyte-specific genes and lipogenic enzymes (such as *FABP4*) and by accumulation of intracellular lipids, the amount of which determines the adipocyte size (*17*). We (*18*) and others (*19*) have shown that there are differences in adipocyte size and tissue biology between different human adipose tissue depots. Here, we demonstrate that the average adipocyte size is smaller in human EpAT and ThAT compared to ScAT, partly due to the presence of larger populations of immature preadipocytes identified by the lower expression of *PPAR-γ*, *CEBPA*, and *FABP4*, and possibly other ongoing biological processes such as inflammation-induced lipolysis (*14*).

It is widely accepted that the balance between the lipid and aqueous phases of adipose tissue is driven by adipocyte size, due to the accumulation of intracellular lipids in large, mature adipocytes (*11*). Here, we demonstrate that this balance

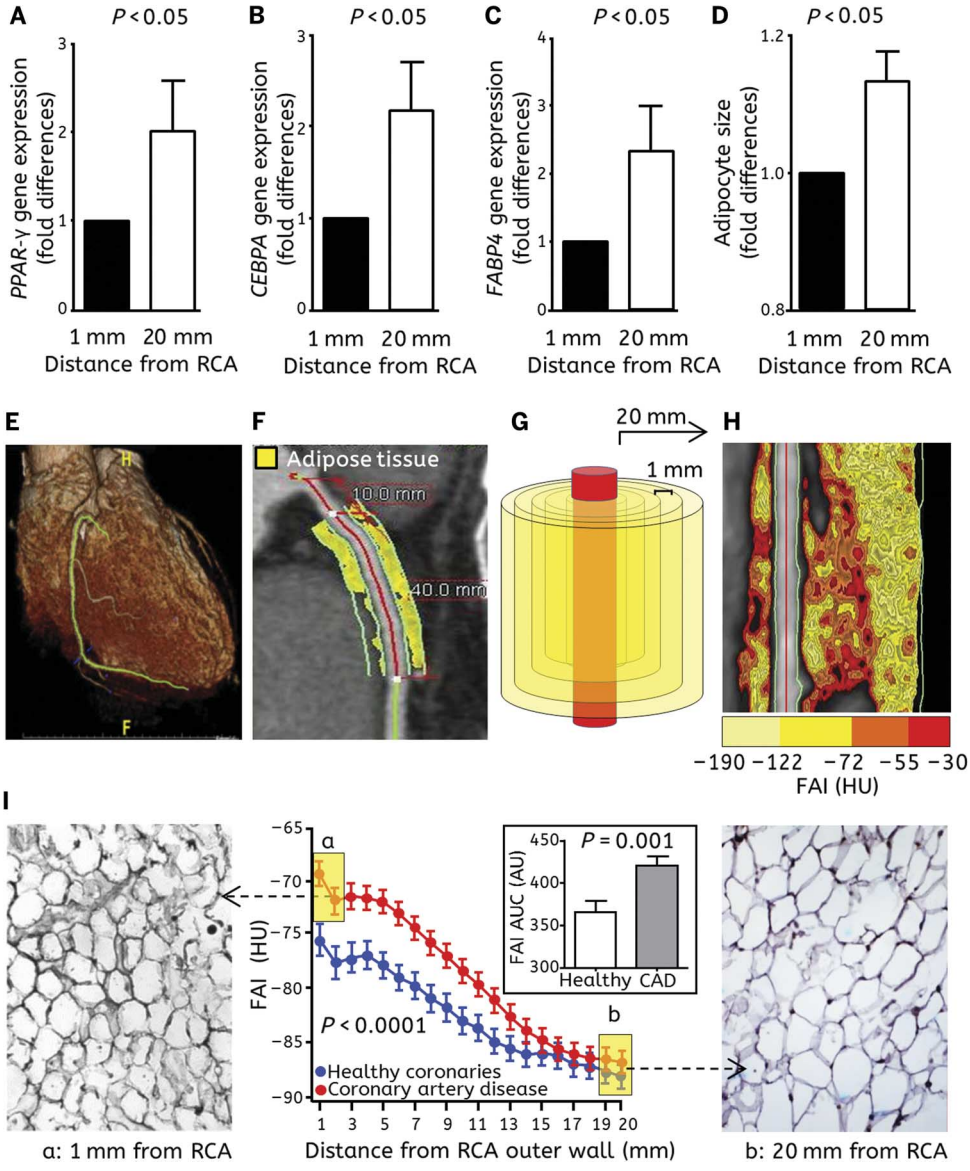

Fig. 7. Gradient of adipocyte size and FAI around the human coronaries in the presence or absence of coronary atherosclerosis. (**A**) *PPAR*-γ, (**B**) *CEBPA*, and (**C**) *CEBPA4* gene expression and (**D**) adipocyte size in pericoronary adipose tissue samples attached to the RCA and paired samples ~20 mm away from it [n = 6 to 12 pairs for (A) to (D)]. (**E** to **G**) In study arm 3, FAI around the RCA of patients undergoing CTA was calculated for each cylindrical 1-mm-thick layer of pericoronary tissue, whereas for a radial distance, FAI was calculated from RCA wall 1 to 20 mm. (**H**) FAI mapping of PVAT around the RCA. (**I**) FAI and radial distance from vascular wall in patients with CAD (n = 149) versus healthy individuals (n = 117) [comparison of the area under the curve (AUC) using unpaired t test and comparison of the curves using two-way ANOVA for repeated measures with "FAI × distance" interaction]. P values by Wilcoxon signed-rank test (A to D).

between the lipid and aqueous phases of adipose tissue can be estimated using CTA, by determining the average attenuation coefficient within a predefined radiodensity window (−190 to −30 HU) (*20*). Previously, it has been suggested that fat attenuation of visceral and ScAT depots provides important information, independently of fat volume or classic risk factors, on cardiovascular risk prediction (*20*, *21*). Now, we demonstrate that the average attenuation of adipose tissue (FAI) measured either ex vivo in adipose tissue explants or in vivo in patients undergoing clinical CTA shows an inverse correlation with adipocyte size and the expression of adipogenic markers, such as *FABP4*, driven by the variations in intracellular lipid accumulation. This imaging phenotyping allows not only the characterization of adipocyte size within each adipose tissue depot but also the detection of differences between different depots. Furthermore, validation of FAI_{ScAT} against in vivo ^{18F}FDG uptake, visualized by PET imaging, suggests that FAI can be used to reliably quantify adipose tissue inflammation, at least in isolated depots, such as ScAT, where adipocyte size is driven by the infiltration of activated macrophages, insulin resistance, or other local tissue biology. FAI may have major applications in endocrinology, because adipocyte size and adipose tissue inflammation are important features of metabolic syndrome, which at present can only be assessed using adipose tissue biopsies or PET/CT, respectively.

In our recent studies (*3*, *8*), we have demonstrated a constant, bidirectional communication between the human arterial wall and its surrounding PVAT, introducing the concept that reverse, "inside-to-outside" signals originating from the vascular wall can affect the biology of PVAT in a paracrine manner. A previous study in mice has also shown that endovascular wire injury induces *PPAR*-γ–mediated phenotypic changes in PVAT, dependent on vascular TNF-α expression (*13*). On the basis of these findings, we now postulate that vascular inflammation may release inflammatory mediators that induce *PPAR*-γ–mediated structural changes in the neighboring PVAT. Our results show that the human arterial wall expresses proinflammatory cytokines, and the inflamed arterial tissue prevents lipid droplet formation in PVAT adipocytes in an ex vivo coculture system by interfering with the ability of human preadipocytes to differentiate, as well as by triggering their proliferation.

Vascular inflammation is a key feature in atherogenesis, because it precedes the formation of atherosclerotic plaques (*1*). Despite the importance of vascular inflammation as a therapeutic target (*22*, *23*), there are no reliable biomarkers to identify patients with high coronary inflammatory burden, because circulating inflammatory biomarkers are not specific and imaging modalities offer information only on the structural changes of the vascular wall. Clinical association studies have previously shown that inflammation of PVAT around the coronary arteries is increased in the presence of atherosclerosis, and it was conventionally believed that PVAT exerts a detrimental effect on the human coronaries, inducing atherogenesis (*24*, *25*). Attention was also focused on linking volume (*26*) or inflammatory status (*27*) of PVAT with the presence of atherosclerotic plaques, whereas recent

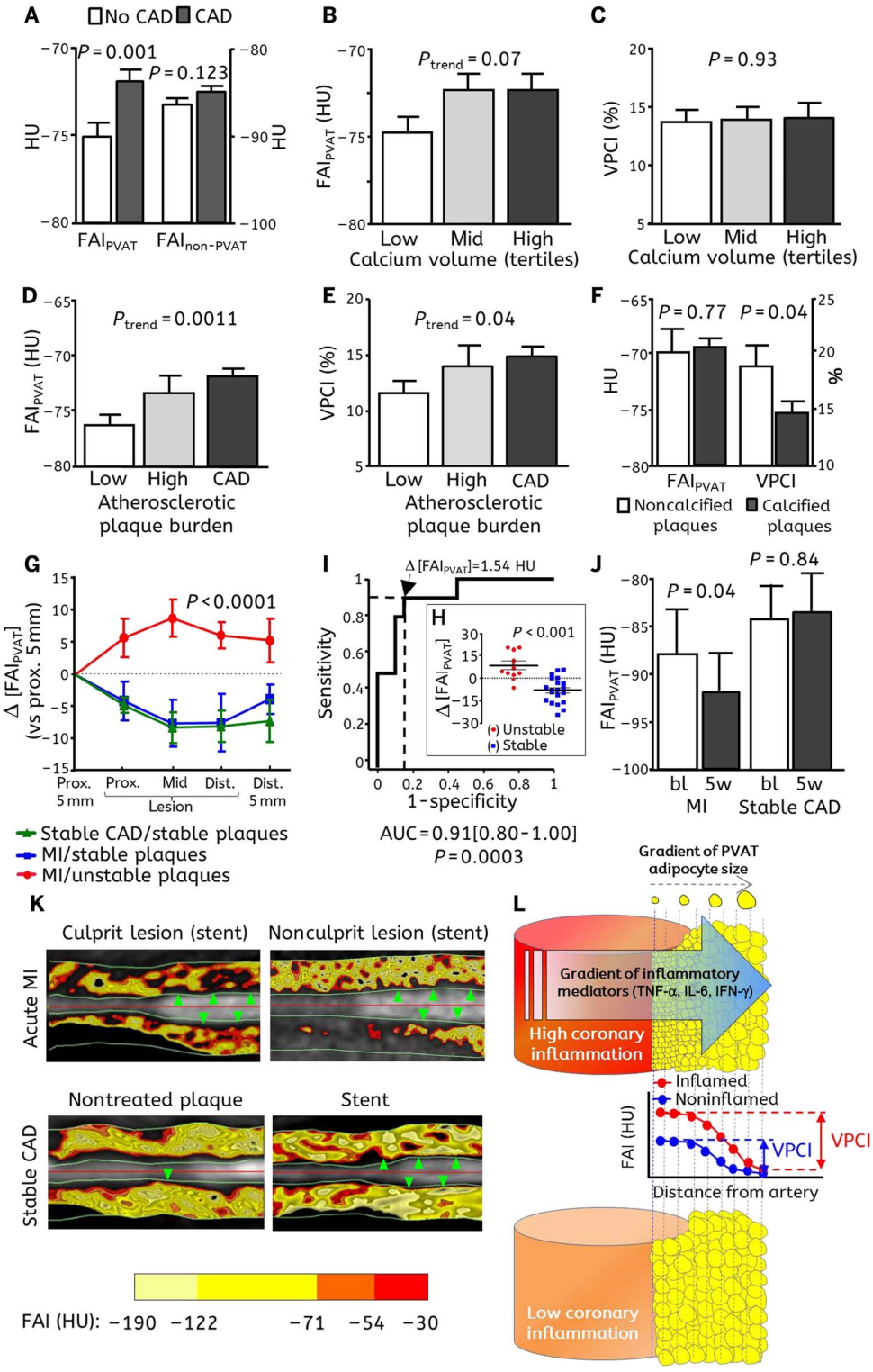

Fig. 8. FAI_{PVAT} and VPCI as novel phenotyping tools for vascular disease. (**A**) Associations between FAI_{PVAT}/$FAI_{non\text{-}PVAT}$ and CAD. (**B** and **C**) Association between calcification volume and FAI_{PVAT} or VPCI. (**D** and **E**) Both FAI_{PVAT} and VPCI are related with atherosclerotic plaque burden in RCA [n = 267 for (A) to (E)]. (**F**) Comparisons of FAI_{PVAT} and VPCI between noncalcified plaques (n = 26) and mixed or calcified plaques (n = 84) in CAD patients with high atherosclerotic plaque burden in the RCA (defined as >33rd percentile). (**G**) Changes in FAI_{PVAT} around ruptured (culprit) atherosclerotic lesions (n = 10) of acute MI patients, nonculprit lesions of the same patients (n = 7), or lesions in stable CAD patients (n = 13); $\Delta[FAI_{PVAT}] = FAI_{PVAT(around\ lesion)} - FAI_{PVAT(proximal\ segment)}$. (**H**) Comparison of $\Delta[FAI_{PVAT}]$ between stable and unstable plaques and (**I**) its diagnostic accuracy in receiver operator characteristic (ROC) curve analysis for detection of unstable plaques (culprit lesions). (**J**) Paired CT scans with 5 weeks difference, to assess temporal changes of FAI_{PVAT} in acute MI and stable CAD patients (n = 5). (**K**) Representative images of FAI_{PVAT} color maps around: (i) a culprit lesion (green arrowheads, identified by the presence of the stent, upper left image), (ii) a nonculprit lesion from the same patient (identified by the presence of the stent implanted in the same session as the culprit, upper right image), (iii) a stable atherosclerotic lesion without a stent (lower left image), and (iv) a stent implanted at least 3 months before imaging (lower right image); green arrowheads flag the plaque/stent. (**L**) A schematic representation of the study's findings that translate the inside-to-outside signal from the human coronaries to their PVAT into an imaging application. P values derived from unpaired t test (A, F, and H), one-way ANOVA (B to E), two-way ANOVA (G), or Wilcoxon signed-rank test (J).

studies by Alam and co-workers (*28*) have also linked EpAT thickness with coronary microvascular function in patients with nonobstructive CAD and EpAT volume with coronary calcification and presence of noncalcified plaques (*29*). However, if vascular inflammation sends paracrine signals to PVAT to prevent lipid accumulation in adipocytes (*3*, *8*, *13*), then this could lead to increased FAI_{PVAT} around inflamed coronary arteries, potentially detectable in vivo. First, we have demonstrated that there is a gradient in adipocyte size and the expression of adipogenic genes (*FABP4*, *CEBPA*, and *PPAR-γ*) moving from PVAT adjacent to the human coronary arteries to adipose tissue further away. Second, we developed new imaging tools that enabled us to analyze FAI_{PVAT} in sequential cylindrical layers around the human coronary arteries, showing a parallel shift of FAI_{PVAT} to more negative values moving away from the vascular wall, reflective of the increase in adipocyte size/adipose tissue lipid content. FAI_{PVAT} was positively related to total atherosclerotic plaque burden and the presence of noncalcified (inflamed) atherosclerotic plaques in the underlying coronary artery because it flags the proinflammatory stimulation of pericoronary adipose tissue as the result of vascular inflammation. Furthermore, we

demonstrate that FAI_{PVAT} is increased around ruptured coronary atherosclerotic plaques of patients scanned during the acute phase of MI after stenting, possibly also due to the contribution of inflammatory cells infiltrating the perivascular space (*30*), a phenomenon that starts to resolve 5 weeks after the event. This latter finding suggests that FAI_{PVAT} may be used to noninvasively detect vulnerable atherosclerotic plaques, thereby enabling the identification of high-risk patients. Our findings imply that the previously reported (*20*, *21*) negative associations of CT attenuation of visceral adipose tissue or ScAT with cardiometabolic risk are explained by the fact that FAI in these depots describes increased adipocyte lipid accumulation; therefore, it can be driven by other cardiometabolic risk factors such as visceral obesity and insulin resistance. On the contrary, FAI_{PVAT} is positively associated with atherosclerotic plaque burden but not with systemic insulin resistance, suggesting that it is driven by local inflammatory stimuli coming from the vascular wall, rather than systemic metabolic conditions such as insulin resistance.

The main limitation of this study is the lack of data demonstrating a predictive value of these imaging markers for clinical outcomes, which falls beyond the scope of this current work. Moreover, the absolute values of FAI need to be tested and validated across different CT scanners in different centers before the markers described in this study become clinical applications.

In conclusion, the existing biomarkers with predictive value in CAD, such as CCS, have major weaknesses given that they do not change with interventions that modify cardiovascular risk and that they represent permanent structural changes in the vascular wall. To track vascular inflammation in early disease states, we now introduce the concept that inflammation in the human coronaries drives changes in the surrounding PVAT in a paracrine manner, leading to less perivascular lipid accumulation closer to the vascular wall. We then describe a method and metrics of imaging phenotyping (FAI_{PVAT} and VPCI) that enable reliable tracking of these changes in adipocyte lipid content/size around the human coronary arteries. The ability of these imaging tools to describe coronary atherosclerosis is independent of any cardiovascular risk factor or other established imaging biomarkers. The FAI_{PVAT} and VPCI may enable early detection of vascular inflammation and have the advantage of being dynamic (they alter with changes in vascular inflammation), which is a major advantage over CCS. We also provide a tool that enables noninvasive detection of vulnerable (highly inflamed) atherosclerotic plaques in the human coronary arteries. This approach can be used to analyze historical CTAs that have previously been performed in patients for diagnostic purposes. If the potential prognostic value of this new imaging phenotyping approach of PVAT is confirmed in clinical studies with prospective follow-up, then it could have a major impact on risk stratification and clinical management of individuals in both primary and secondary prevention.

MATERIAL AND METHODS

Study design

The objective of this study was to develop a methodology for the detection of vascular inflammation in human coronary arteries, by performing functional imaging of coronary PVAT using CTA. This study (i) links molecular phenotyping of human PVAT with its CT imaging characteristics ex vivo and in vivo, (ii) develops a method that links CT attenuation of human adipose tissue with lipid accumulation and tissue inflammation, and (iii) develops a method that uses molecular phenotyping and CT attenuation of PVAT around the human coronaries, as a means to quantify vascular inflammation related with atherosclerotic disease burden and plaque vulnerability in clinical cohorts.

Study arm 1 consisted of 453 patients undergoing cardiac surgery at the Oxford University Hospitals NHS Foundation Trust (table S1). Adipose tissue samples (ThAT, n = 417; ScAT, n = 374; EpAT, n = 264) were harvested during surgery for gene expression studies, histology, and CT imaging as explants. A subgroup of 105 patients also underwent CTA to link the histological and biological characteristics of the adipose tissue biopsies with the imaging characteristics of the same adipose tissue depots in vivo and in vitro. Study arm 2 included 45 patients undergoing CABG (table S1) for mechanistic experiments and PVAT phenotyping. Study arm 3 included a clinical cohort of 273 patients who underwent diagnostic coronary CTA (table S3) to validate the findings generated from study arms 1 and 2 and translate them in a clinical setting. Study arm 4 included 22 patients with CAD (table S3) undergoing CTA to assess whether FAI_{PVAT} can identify unstable coronary plaques.

The study was conducted according to Declaration of Helsinki principles and approved by the local Research Ethics Committee (Oxford REC C 11/SC/0140, Oxford REC C 15/SC/0545, and Hippokration Hospital ID 2.2.15/1654 for study arm 4).

Blood sampling and measurements of circulating biomarkers

Fasting venous blood samples were obtained from the patients in study arm 1 before cardiac surgery. Serum insulin was measured by chemiluminescent microparticle immunoassay, and serum glucose was measured by the hexokinase method using commercial kits (ABBOTT). Insulin resistance was defined by HOMA-IR, calculated using the formula (glucose × insulin)/405, with glucose measured in milligrams per deciliter and insulin in milliunits per liter.

Imaging studies using CT and PET/CT

Details on CT and PET/CT imaging studies of adipose tissue, PVAT, and coronary plaque characterization are presented in the Supplementary Materials. Technical considerations on the calculation of the new imaging biomarkers FAI_{PVAT} and VPCI are presented in fig. S12.

Adipose tissue characterization by CT

Adipose tissue was defined as all voxels with attenuation between −190 and −30 HU. Voxel attenuation histograms were plotted, and the FAI was defined as the average attenuation of the adipose tissue volume of interest (within the prespecified window of −190 to −30 HU; see the Supplementary Materials for further details).

PVAT characterization

Perivascular tissue around the RCA was segmented into 20 concentric cylindrical 1-mm-thick layers, extending between the first and fifth centimeter from its ostium, and FAI was calculated for each layer. The FAI curves of adipose tissue were plotted against the radial distance from the outer vascular wall (see the Supplementary Materials for further details).

FAI of PVAT

FAI_{PVAT} was defined as the FAI of adipose tissue in a layer of tissue within a radial distance from the outer coronary artery wall equal to the average diameter of the tracked RCA segment. Non-PVAT FAI ($FAI_{non\text{-}PVAT}$) was defined at the most distal concentric layer of adipose tissue from RCA wall. VPCI was then calculated as the % change in FAI from PVAT (FAI_{PVAT}) to non-PVAT (2 cm away from the RCA's outer wall, $FAI_{non\text{-}PVAT}$), as defined above (VPCI = $[100 \times (FAI_{PVAT} - FAI_{non\text{-}PVAT})/|FAI_{PVAT}|]$); see the Supplementary Materials for further details.

Coronary plaque analysis using CTA

Coronary plaques between 65 and 265 HU were described as fibrous, and coronary plaques more than 465 HU were described as calcified. Atherosclerotic plaque burden was calculated as the ratio of fibrous plaque volume to total vessel volume (see the Supplementary Materials for further details).

Statistical analysis

Continuous variables were tested for normal distribution using the Kolmogorov-Smirnov test. Non-normally distributed variables are presented as median (25th to 75th percentile) and whiskers (Tukey). Normally distributed variables are presented as means ± SEM. Between-group comparisons of continuous variables were performed using unpaired *t* test (for two groups) or one-way ANOVA (or Kruskal-Wallis as appropriate) for three groups followed by Bonferroni (or Dunn's) post hoc correction for multiple comparisons, as indicated. Paired comparisons were performed using paired *t* test (or Wilcoxon signed-rank test), and for three or more groups, repeated-measures ANOVA (or Friedman's test as appropriate) was used. For between-group serial changes, we used two-way ANOVA for repeated measures with interaction terms as presented in the figure legends. Categorical variables were compared by using χ^2 test. Correlations between continuous variables were assessed by using bivariate analysis, and Pearson's *r* or Spearman's ρ coefficient was estimated, as indicated in the figure legends.

To test whether FAI_{PVAT} is related with the presence of CAD, we performed multivariable logistic regression for predictors of obstructive CAD (>50% stenosis of the lumen) and multivariate linear regression for atherosclerotic plaque burden in the RCA (independent variables as described in relevant text sections and table S4). The results of the regression analysis are presented as standardized β and *P* values. All statistical tests were performed using SPSS version 20.0, and $P < 0.05$ was considered statistically significant. Individual subject-level data are reported in table S5.

SUPPLEMENTARY MATERIALS

www.sciencetranslationalmedicine.org/cgi/content/full/9/398/eaal2658/DC1

Materials and Methods

Fig. S1. Study flow chart.

Fig. S2. Adipocyte differentiation in vitro and lipid accumulation.

Fig. S3. Effects of proinflammatory cytokines on preadipocyte differentiation.

Fig. S4. FAI and macrophage infiltration and polarization status in adipose tissue explants.

Fig. S5. Gene expression of inflammatory cytokines and markers of macrophage infiltration/polarization in coronary PVAT versus non-PVAT.

Fig. S6. Variation in FAI mapping of pericoronary adipose tissue in the absence of vascular disease.

Fig. S7. FAI_{PVAT} and CAD.

Fig. S8. Associations between EpAT and PVAT volumes and coronary atherosclerosis/calcification.

Fig. S9. Associations between coronary PVAT imaging phenotyping and coronary calcium score.

Fig. S10. Correlations between FAI_{PVAT} and coronary plaque burden in major epicardial arteries.

Fig. S11. Detection of noncalcified plaques in human coronaries by CT imaging mapping of pericoronary adipose tissue.

Fig. S12. Technical considerations related to calculation of FAI.

Table S1. Demographic characteristics of study participants.

Table S2. Range of FAI values in adipose tissue explants and in vivo.

Table S3. Demographic characteristics of study participants in study arms 3 and 4.

Table S4. Predictive value of FAI_{PVAT} to describe CAD and atherosclerotic plaque burden independently of coronary calcium score.

Table S5. Individual subject-level data.

REFERENCES AND NOTES

1. R. Ross, Atherosclerosis—an inflammatory disease. *N. Engl. J. Med.* **340**, 115–126 (1999).
2. R. Lee, M. Margaritis, K. M. Channon, C. Antoniades, Evaluating oxidative stress in human cardiovascular disease: Methodological aspects and considerations. *Curr. Med. Chem.* **19**, 2504–2520 (2012).
3. M. Margaritis, A. S. Antonopoulos, J. Digby, R. Lee, S. Reilly, P. Coutinho, C. Shirodaria, R. Sayeed, M. Petrou, R. De Silva, S. Jalilzadeh, M. Demosthenous, C. Bakogiannis, D. Tousoulis, C. Stefanadis, R. P. Choudhury, B. Casadei, K. M. Channon, C. Antoniades, Interactions between vascular wall and perivascular adipose tissue reveal novel roles for adiponectin in the regulation of endothelial nitric oxide synthase function in human vessels. *Circulation* **127**, 2209–2221 (2013).
4. T. Christen, Y. Sheikine, V. Z. Rocha, S. Hurwitz, A. B. Goldfine, M. Di Carli, P. Libby, Increased glucose uptake in visceral versus subcutaneous adipose tissue revealed by PET imaging. *JACC Cardiovasc. Imaging* **3**, 843–851 (2010).
5. P. Greenland, L. LaBree, S. P. Azen, T. M. Doherty, R. C. Detrano, Coronary artery calcium score combined with Framingham score for risk prediction in asymptomatic individuals. *JAMA* **291**, 210–215 (2004).
6. I. E. Hoefer, S. Steffens, M. Ala-Korpela, M. Bäck, L. Badimon, M.-L. Bochaton-Piallat, C. M. Boulanger, G. Caligiuri, S. Dimmeler, J. Egido, P. C. Evans, T. Guzik, B. R. Kwak, U. Landmesser, M. Mayr, C. Monaco, G. Pasterkamp, J. Tuñón, C. Weber; ESC Working Group Atherosclerosis and Vascular Biology, Novel methodologies for biomarker discovery in atherosclerosis. *Eur. Heart J.* **36**, 2635–2642 (2015).
7. C. Antoniades, A. S. Antonopoulos, D. Tousoulis, C. Stefanadis, Adiponectin: From obesity to cardiovascular disease. *Obes. Rev.* **10**, 269–279 (2009).
8. A. S. Antonopoulos, M. Margaritis, P. Coutinho, C. Shirodaria, C. Psarros, L. Herdman, F. Sanna, R. De Silva, M. Petrou, R. Sayeed, G. Krasopoulos, R. Lee, J. Digby, S. Reilly, C. Bakogiannis, D. Tousoulis, B. Kessler, B. Casadei, K. M. Channon, C. Antoniades, Adiponectin as a link between type 2 diabetes and vascular NADPH oxidase activity in the human arterial wall: The regulatory role of perivascular adipose tissue. *Diabetes* **64**, 2207–2219 (2015).
9. J. M. Ntambi, K. Young-Cheul, Adipocyte differentiation and gene expression. *J. Nutr.* **130**, 3122S–3126S (2000).
10. J. Bassols, F. J. Ortega, J. M. Moreno-Navarrete, B. Peral, W. Ricart, J.-M. Fernández-Real, Study of the proinflammatory role of human differentiated omental adipocytes. *J. Cell. Biochem.* **107**, 1107–1117 (2009).
11. M. DiGirolamo, J. L. Owens, Water content of rat adipose tissue and isolated adipocytes in relation to cell size. *Am. J. Physiol.* **231**, 1568–1572 (1976).
12. C. Farnier, S. Krief, M. Blache, F. Diot-Dupuy, G. Mory, P. Ferre, R. Bazin, Adipocyte functions are modulated by cell size change: Potential involvement of an integrin/ERK signalling pathway. *Int. J. Obes. Relat. Metab. Disord.* **27**, 1178–1186 (2003).
13. M. Takaoka, H. Suzuki, S. Shioda, K. Sekikawa, Y. Saito, R. Nagai, M. Sata, Endovascular injury induces rapid phenotypic changes in perivascular adipose tissue. *Arterioscler. Thromb. Vasc. Biol.* **30**, 1576–1582 (2010).
14. R. W. Grant, J. M. Stephens, Fat in flames: Influence of cytokines and pattern recognition receptors on adipocyte lipolysis. *Am. J. Physiol. Endocrinol. Metab.* **309**, E205–E213 (2015).
15. M.-J. Lee, Y. Wu, S. K. Fried, A modified protocol to maximize differentiation of human preadipocytes and improve metabolic phenotypes. *Obesity (Silver Spring)* **20**, 2334–2340 (2012).
16. N. Franck, K. G. Stenkula, A. Öst, T. Lindström, P. Strålfors, F. H. Nystrom, Insulin-induced GLUT4 translocation to the plasma membrane is blunted in large compared with small primary fat cells isolated from the same individual. *Diabetologia* **50**, 1716–1722 (2007).
17. M. R. Kazemi, C. M. McDonald, J. K. Shigenaga, C. Grunfeld, K. R. Feingold, Adipocyte fatty acid–binding protein expression and lipid accumulation are increased during activation of murine macrophages by toll-like receptor agonists. *Arterioscler. Thromb. Vasc. Biol.* **25**, 1220–1224 (2005).
18. A. S. Antonopoulos, M. Margaritis, P. Coutinho, J. Digby, R. Patel, C. Psarros, N. Ntusi, T. D. Karamitsos, R. Lee, R. De Silva, M. Petrou, R. Sayeed, M. Demosthenous, C. Bakogiannis, P. B. Wordsworth, D. Tousoulis, S. Neubauer, K. M. Channon, C. Antoniades, Reciprocal effects of systemic inflammation and brain natriuretic peptide on adiponectin biosynthesis in adipose tissue of patients with ischemic heart disease. *Arterioscler. Thromb. Vasc. Biol.* **34**, 2151–2159 (2014).
19. C. Bambace, A. Sepe, E. Zoico, M. Telesca, D. Olioso, S. Venturi, A. Rossi, F. Corzato, S. Faccioli, L. Cominacini, F. Santini, M. Zamboni, Inflammatory profile in subcutaneous and epicardial adipose tissue in men with and without diabetes. *Heart Vessels* **29**, 42–48 (2014).
20. K. J. Rosenquist, A. Pedley, J. M. Massaro, K. E. Therkelsen, J. M. Murabito, U. Hoffmann, C. S. Fox, Visceral and subcutaneous fat quality and cardiometabolic risk. *JACC Cardiovasc. Imaging* **6**, 762–771 (2013).

21. T. M. Abraham, A. Pedley, J. M. Massaro, U. Hoffmann, C. S. Fox, Association between visceral and subcutaneous adipose depots and incident cardiovascular disease risk factors. *Circulation* **132**, 1639–1647 (2015).
22. D. Tousoulis, C. Psarros, M. Demosthenous, R. Patel, C. Antoniades, C. Stefanadis, Innate and adaptive inflammation as a therapeutic target in vascular disease: The emerging role of statins. *J. Am. Coll. Cardiol.* **63**, 2491–2502 (2014).
23. A. S. Antonopoulos, M. Margaritis, R. Lee, K. Channon, C. Antoniades, Statins as anti-inflammatory agents in atherogenesis: Molecular mechanisms and lessons from the recent clinical trials. *Curr. Pharm. Des.* **18**, 1519–1530 (2012).
24. S. N. Verhagen, M. P. Buijsrogge, A. Vink, L. A. van Herwerden, Y. van der Graaf, F. L. J. Visseren, Secretion of adipocytokines by perivascular adipose tissue near stenotic and non-stenotic coronary artery segments in patients undergoing CABG. *Atherosclerosis* **233**, 242–247 (2014).
25. S. N. Verhagen, F. L. J. Visseren, Perivascular adipose tissue as a cause of atherosclerosis. *Atherosclerosis* **214**, 3–10 (2011).
26. P. Maurovich-Horvat, K. Kallianos, L.-C. Engel, J. Szymonifka, C. S. Fox, U. Hoffmann, Q. A. Truong, Influence of pericoronary adipose tissue on local coronary atherosclerosis as assessed by a novel MDCT volumetric method. *Atherosclerosis* **219**, 151–157 (2011).
27. M. Konishi, S. Sugiyama, Y. Sato, S. Oshima, K. Sugamura, T. Nozaki, K. Ohba, J. Matsubara, H. Sumida, Y. Nagayoshi, K. Sakamoto, D. Utsunomiya, K. Awai, H. Jinnouchi, Y. Matsuzawa, Y. Yamashita, Y. Asada, K. Kimura, S. Umemura, H. Ogawa, Pericardial fat inflammation correlates with coronary artery disease. *Atherosclerosis* **213**, 649–655 (2010).
28. M. S. Alam, R. Green, R. de Kemp, R. S. Beanlands, B. J. W. Chow, Epicardial adipose tissue thickness as a predictor of impaired microvascular function in patients with non-obstructive coronary artery disease. *J. Nucl. Cardiol.* **20**, 804–812 (2013).
29. N. Alexopoulos, D. S. McLean, M. Janik, C. D. Arepalli, A. E. Stillman, P. Raggi, Epicardial adipose tissue and coronary artery plaque characteristics. *Atherosclerosis* **210**, 150–154 (2010).
30. E. Henrichot, C. E. Juge-Aubry, A. Pernin, J.-C. Pache, V. Velebit, J.-M. Dayer, P. Meda, C. Chizzolini, C. A. Meier, Production of chemokines by perivascular adipose tissue: A role in the pathogenesis of atherosclerosis? *Arterioscler. Thromb. Vasc. Biol.* **25**, 2594–2599 (2005).

Acknowledgments: We are grateful to M. N. Kararoudi for his support in the analysis of part of the ex vivo images of adipose tissue explants. **Funding:** The study was funded by the British Heart Foundation (BHF) (FS/16/15/32047 and PG/13/56/30383 to C.A.), the BHF Centre of Research Excellence (Oxford) (RE/08/004 to M.M. and C.A.), the National Institute for Health Research–Oxford Biomedical Research Centre, the European Commission (Marie Curie ITN RADOX GA316738 and IF REDO$_X$HEART GA656990), and the NovoNordisk Foundation (NNF15CC0018486). **Author contributions:** A.S.A. participated in patient recruitment, clinical data and biological sample collection, data analysis, statistical analysis, and writing of the manuscript. F.S., M.M., C.P., and P.C. performed experiments and data analysis and reviewed the manuscript. N.S. participated in clinical data collection. S.T. participated in clinical data collection and data analysis. L.H. participated in patient recruitment and data analysis. I.A. performed experiments. C.S. participated in clinical data collection and reviewed the manuscript. E.K.O. participated in clinical data collection and image/data analysis. A.-M.K. and C.M.B. participated in data analysis. M.P., R.S., and G.K. contributed to participant recruitment and biological sample collection. A.K., R.U., S. Anthony, N.A., and D.T. contributed to clinical data collection. J.D., S. Achenbach, S.N., and K.M.C. provided advice and discussed and reviewed the manuscript. C.A. designed the study, raised the funding, coordinated and directed the project, and wrote the manuscript. **Competing interests:** The method for analysis of perivascular FAI and the VPCI described in this article is subject to a UK patent application, number 1414496.8. C.A., K.M.C., S.N., and C.S. are founders and shareholders of Caristo Diagnostics, a CT image analysis spinout company of the University of Oxford. **Data and materials availability:** All data are included in the paper or the Supplementary Materials. For any further information, please contact C.A.

Submitted 31 October 2016
Resubmitted 30 January 2017
Accepted 30 May 2017
Published 12 July 2017
10.1126/scitranslmed.aal2658

Citation: A. S. Antonopoulos, F. Sanna, N. Sabharwal, S. Thomas, E. K. Oikonomou, L. Herdman, M. Margaritis, C. Shirodaria, A.-M. Kampoli, I. Akoumianakis, M. Petrou, R. Sayeed, G. Krasopoulos, C. Psarros, P. Ciccone, C. M. Brophy, J. Digby, A. Kelion, R. Uberoi, S. Anthony, N. Alexopoulos, D. Tousoulis, S. Achenbach, S. Neubauer, K. M. Channon, C. Antoniades, Detecting human coronary inflammation by imaging perivascular fat. *Sci. Transl. Med.* **9**, eaal2658 (2017).

Science Translational Medicine

Detecting human coronary inflammation by imaging perivascular fat

Alexios S. Antonopoulos, Fabio Sanna, Nikant Sabharwal, Sheena Thomas, Evangelos K. Oikonomou, Laura Herdman, Marios Margaritis, Cheerag Shirodaria, Anna-Maria Kampoli, Ioannis Akoumianakis, Mario Petrou, Rana Sayeed, George Krasopoulos, Constantinos Psarros, Patricia Ciccone, Carl M. Brophy, Janet Digby, Andrew Kelion, Raman Uberoi, Suzan Anthony, Nikolaos Alexopoulos, Dimitris Tousoulis, Stephan Achenbach, Stefan Neubauer, Keith M. Channon and Charalambos Antoniades

Sci Transl Med **9**, eaal2658.
DOI: 10.1126/scitranslmed.aal2658

Picturing plaques and imaging inflammation

To determine risk of future coronary artery disease, calcium content in vascular plaques is typically evaluated by coronary calcium scoring, which uses computerized tomography (CT) imaging. To detect inflammation and subclinical coronary artery disease (soft, noncalcified plaques), Antonopoulos *et al.* developed an alternative metric called the perivascular CT fat attenuation index (FAI). The perivascular FAI uses CT imaging of adipose tissue surrounding the coronary arteries to assess adipocyte size and lipid content. Larger, more mature adipocytes exhibit greater lipid accumulation, which is inversely associated with the FAI. Inflammation reduces lipid accumulation and slows preadipocyte differentiation. Imaging pericoronary fat in human patients after myocardial infarction revealed that unstable plaques had larger perivascular FAIs than stable plaques and that the FAI was greatest directly adjacent to the inflamed coronary artery. The perivascular FAI may be a useful, noninvasive method for monitoring vascular inflammation and the development of coronary artery disease.